DRAFT VERSION OCTOBER 27, 2014
Preprint typeset using LaTeX style emulateapj v. 12/16/11

PROBING THE INNER KPC OF MASSIVE GALAXIES WITH STRONG GRAVITATIONAL LENSING

YASHAR D. HEZAVEH, PHILIP J. MARSHALL, ROGER D. BLANDFORD
Kavli Institute for Particle Astrophysics and Cosmology, Stanford University, Stanford, CA, USA
Draft version October 27, 2014

ABSTRACT

We examine the prospects of detecting demagnified images of gravitational lenses in observations of strongly lensed mm-wave molecular emission lines with ALMA. We model the lensing galaxies as a superposition of a dark matter component, a stellar population, and a central supermassive black hole and forecast the detection of the central images for a range of relevant parameters (e.g. stellar core and black hole mass). We find that over a large range of acceptable parameters, future deep observations of lensed molecular lines with ALMA will be able to detect the central images at $\gtrsim 3\sigma$ significance. We use Fisher analysis to examine the constraints that could be placed on these parameters in various scenarios.

Subject headings: black hole physics — gravitational lensing: strong — galaxies: formation — galaxies: high-redshift

1. INTRODUCTION

Probing the matter distribution in the innermost kpc of galaxies can answer key questions about super massive black holes (SMBH), galaxy formation, and dark matter. It is now established that almost every massive galaxy harbors a SMBH at its center with a mass that strongly correlates with the mass of the host galaxy (Kormendy & Richstone 1995; Ferrarese & Merritt 2000; Gebhardt et al. 2000; Tremaine et al. 2002). In addition, the distribution of stellar populations in central regions of galaxies contains information about their past merger histories and SMBH-stellar population interactions. (e.g Barnes & Hernquist 1992; Ebisuzaki et al. 1991). Various dark matter models also predict different structures for the central regions of dark matter halos (e.g Rocha et al. 2013). Mapping the matter density in the central regions of galaxies can thus shed light on various astrophysical phenomena.

Morphological studies of galaxies in optical wavelengths have shown that, unlike their lower-mass counterparts, the most massive elliptical galaxies often exhibit cored stellar light profiles, with core sizes ranging from 50 to 500 pc (e.g., Ferrarese et al. 2006). These galaxies are thought to form through gas-poor mergers. In such mergers, the central structure of the resulting galaxy is dominated by the inner structure of the more concentrated progenitor. Since high-mass ellipticals are thought to form from mergers of their lower-mass counterparts, with steep profiles, the existence of cores in these galaxies represents a challenge to our understanding of galaxy mergers. Cores in massive ellipticals, therefore, should be the result of different (not merger) mechanisms. "Black hole scouring" is currently the only known plausible mechanism that could explain core-formation in these galaxies (Thomas et al. 2014).

It is thought that during a merger, the SMBHs of the two merging galaxies form a binary which sinks to the center of the potential. The two orbiting SMBHs then dissipate angular momentum through three-body interactions with nearby central stars, pushing them to higher orbits and scouring out a core. This angular momentum loss then allows the two black holes to merge (Begelman et al. 1980). Previous studies have shown that the core sizes in these galaxies scales with the mass of their SMBHs, in agreement with theoretical predictions (Kormendy & Bender 2009; Kormendy & Ho 2013). Such measurements, however have been limited to low redshifts, since both dynamical measurements to constrain the stellar and SMBH masses, and morphological measurements to constrain core sizes require very high physical resolutions.

Strong gravitational lensing is a powerful tool for probing matter distribution in distant galaxies. Among other things, strong lenses have been used to constrain galaxy masses (e.g.), density profiles (e.g.), and abundance of dark matter subhalos (e.g.). Strong lensing formalism indicates that the number of lensed images should always be odd. For double and quad image configurations, a third and a fifth image are predicted to exist near the centers of lensing galaxies. Unlike the other lensed images, which are magnified, this image can be significantly *demagnified*, making its detection difficult. It is well-understood that the magnification of the central images is very sensitive to the matter distribution in the innermost regions of lens galaxies: very steep singular density profiles significantly demagnify the central images, whereas cored or shallow profiles render them brighter. In addition to their low flux, the fact that central images coincide with the emission from lens galaxies makes their detection even harder. If observed in optical, absorption in the central dense regions of the lens make the central images even dimmer, while the photon noise from the lens emission further reduces the sensitivity. Moreover, distinguishing the central images from emission originating in the lens galaxies is extremely challenging.

needs work The individual behavior () and statistical properties of central images in lens populations have been extensively studied (e.g. Wallington & Narayan 1993; Evans & Hunter 2002; Keeton 2003), suggesting that central images could have a wide range of magnifications. Observational searches for these images have found a number of candidates (e.g. Inada et al. 2005), however, only one secure detections of a central image of a galaxy-scale lens exists to date (Winn et al. 2004).(Inada:08 is a cluster?) To avoid the possibility of absorption in the lens, most studies have focused on strongly lensed radio quasars and the radio spectrum of candidate central images have been used to distinguish them from faint emission from the lens galaxies.

A new large population of strong lenses has recently been discovered. These systems were initially detected as bright point sources in wide area mm/submm surveys (Vieira et al. 2010; Negrello et al. 2010). Follow-up observations have confirmed that they constitute a large population of strong lenses (Vieira et al. 2013; Hezaveh et al. 2013; Bussmann et al. 2013). In particular, ALMA observations of these sources have revealed that the background galaxies are starburst, high redshift galaxies, containing a wealth of cold molecular gas (Weiß et al. 2013). These observations showed that the extreme brightness the sources in combination with the high sensitivity of ALMA results in very high signal to noise ratios (e.g. the

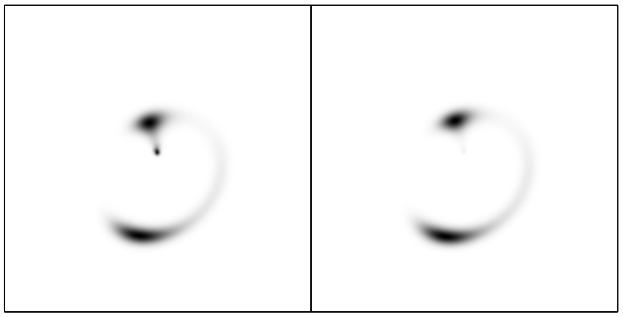

FIG. 1.— illustration of the central image in 2 cases:

lens models in Hezaveh et al. 2013, were based on $\sim$ 50 second long observations). Motivated by the discovery of this population and the operation of ALMA, here we revisit the issue of detecting central images. Deep ALMA observations of molecular lines in these sources are likely to be carried out for various reasons (e.g., Hezaveh et al. 2014; Hezaveh 2014). If a central image of a lensed molecular line is detected, it will be readily identifiable since it will correspond to the redshift of the source, leaving no doubt about its origin. In addition, since these lines are in mm-bands, the line fluxes are very unlikely to be suppressed due to absorption in the lens.

In this letter, we explore the possibility of detecting the central lensed images in such deep observations and investigate the constraints that could be placed on the core size, mass of SMBHs, and the slope of the density profiles from detection, or non-detection of such images. In Section 2 we describe the simulations, in Section 3 we present the results and discuss them, and finally conclude in Section 4. We use a flat ΛCDM cosmology with $h = 0.71$ and $\Omega_M = 0.267$.

2. SIMULATIONS

We generate lensed images of background sources, predict ALMA visibilities, and use them to estimate the detection significance of central images for various parameters. We simulate observations of a high-J CO line. The line is assumed to have a velocity integrated flux of 1 Jy km/s and a FWHM of 400 km/s, resulting in an average flux of 2.5 mJy over a XX km/s band.

We model the lens potential as a sum of three components: dark matter, stellar population and central SMBH. The dark matter is modeled as a singular power-law with a slope of 0.1, in agreement with the projected surface mass density of the NFW profile (Golse & Kneib 2002). As by pointed out by (Keeton 2003), due to its extreme flatness in these regimes, the dark matter component has negligible influence on the central images. The stellar population is modeled as a a core power-law, $\Sigma \propto (r^2 + s^2)^{\gamma}$. Figure 2 shows the stellar component (red curve), dark matter component (black dashed curve) and the sum of the two (black solid curved). The grey dashed curves show a few example of core-sersic models with parameters taken from Ferrarese et al. (2006). We note that although the cored power-law model used in this work does not account for the slope of the stellar distribution below the core break, it is a close fit and a reasonable model to approximate the observed stellar light profiles. The black hole is modeled as a simple point mass at the center of the potential. In this work we assume that all the three components are concentric.

The lens mass is set to XX $M_{\odot}$ resulting in an Einstein radius of $\sim XX''$, in agreement with galaxy-galaxy strong lenses. We divide this mass equally (in a radius of 10 kpc) between stellar and dark matter.

To predict the visibilities we calculate the ALMA uv-coverage for a 5-hr long observation with the most extended antenna configuration (full array), using the

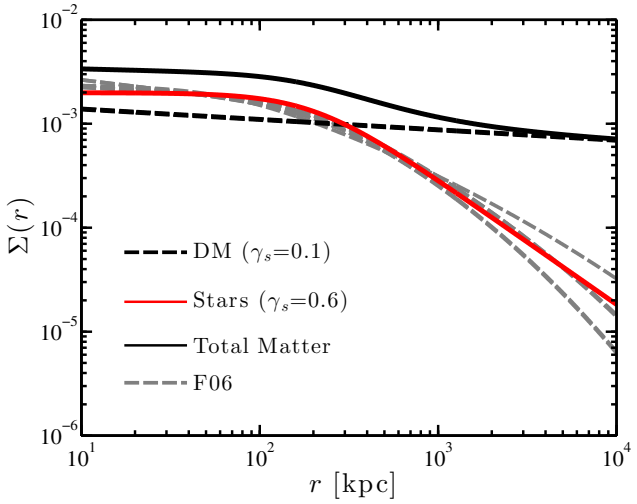

FIG. 2.— Model density profiles. The black dashed line shows the dark matter component, with a slope of 0.1, consistent with a projected NFW at the innermost regions. the grey dashed curves show cored-sersic five fits to stellar light profiles of massive galaxies from Ferrarese 2006. The red solid curve shows our cored-power-law model that we use to approximate this stellar component. The solid black line shows the total matter density (dark plus stellar) of our model.

simobserve task of Common Astronomy Software Applications package, which results in an angular resolution of $\sim$ 20 *milli-arcsec* at an observing frequency of 240 GHz. The visibilities for each channel are calculated by computing the 2D Fourier transform of the corresponding layer of the data cube and resampling the Fourier transform maps over the uv-coverage. The noise is estimated using ALMA sensitivity calculator for a channel width of 8 km/s at 240 GHz. We use finite differencing of visibilities to calculate the Fisher information and the parameter covariance matrix to calculate the significance of black hole mass measurement.

For simulations where we calculate the detection significance of the demagnified image, we compute the magnification at every pixel in the image plane and generate maps with and without the the demagnified flux and evaluate the detection significance of the central image by comparing the two images. In other simulations where the constrains on parameters are needed, we use a Fisher analysis to compute the full covariance of all parameters. We then marginalize over the nuisance parameters (e.g. source position, lens ellipticity) to calculate the marginalized likelihood of the relevant parameters.

3. RESULTS AND DISCUSSIONS

3.1. *Detection of central images*

1) We evaluate the detection significance of central images over a range of relevant parameters.

2) Figure 4 shows our results for a 10-hr long observation with ALMA

3) we show that, as expected, the image is fainter for steeper profile slopes.

4) the 0.9 value (combined with 0.1 DM) results in the isothermal profile, which has been shown to be consistent with strong lensing data

5) if that's the case, and in the absence of massive BHs, then stellar cores as small as $\sim$ 80 pc should allow a

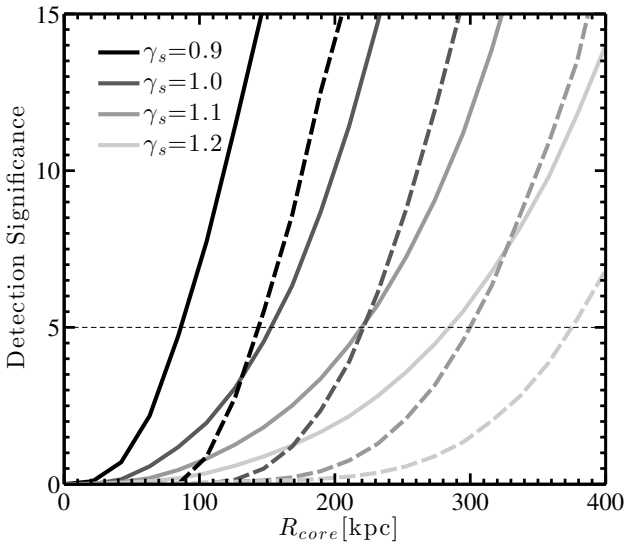

FIG. 3.— Significance of detection of the central image as a function of the stellar core size for a 10-hr long ALMA observation. The colors correspond to different slopes of the stellar component. The solid curves correspond to a case without a SMBH while the dashed line show the result of a simulation which includes a $2 \times 10^8 M_\odot$ SMBH at its center.

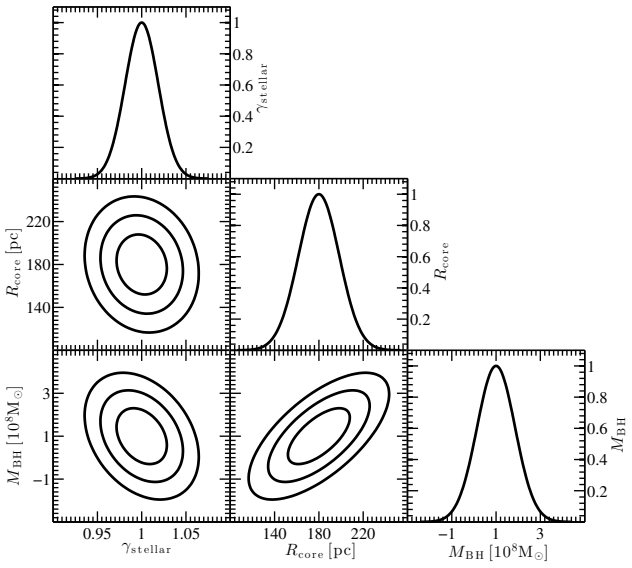

FIG. 4.— Covariance matrix of parameters for a few different scenarios.

5σ detection of the central images.

5A) we note that for much shallower density profiles, the central image is actually *magnified*, and therefore it's detection should be trivial.

6) the flux is significantly supressed by the central SMBH

7) the dashed curves show the same for a galaxy with a $2e8M_\odot$ SMBH.

8) we note that, as pointed out in Keeton 2003, there's a large range of possibilities for plausible lens parameters: although for some parameter combinations (e.g., $\gamma_s = 1.2$, $M_{BH} = 2e8$,$R_{core} < 300pc$) there is no chance of detecting the central image, over a significant fraction of allowed parameters the central image could be detected.

9) to calculate this plot we have used a configuration XX, because: it allows us to resolve the central image (if existent), while it is more sensitive that more extended configurations. In addition, this is the configuration that will be likely used for other projects/sciences.

3.2. *SMBHs and the core size*

1) in this section we study how well we can constrain the mass of the central black hole, the slope of the density and the size of the stellar core.

2) we choose a few models where the central image is detected OR not detected and use a Fisher analysis to determine the degeneracies between the parameters and the detection significance of each parameter.

3) we note that in the Fisher analysis we include all nuisance parameters (e.g. source position, size, etc.) and marginalize over them

4) Figure 4 shows the parameters for a case with R_{core}=180 pc, $M_{BH} = 1e8$ and $\gamma = 1$. As seen from Figure 3, this parameter combination results in a faint ($\sim 3\sigma$) detection of the central image.

5) we note that the black hole mass is degenerate with the core size: a larger core, results in a brighter image, which can be supressed by a more massive BH.

6) The Fisher data show that the black hole mass cannot be measured with high significance in such observations (1.16σ)

7) however, interestingly, the degeneracy of the black hole mass and the size of the central core breaks at the high end. and the stellar core is measured with XX σ

8) this is likely because a very large core results in a fairly extended central images, which could be *resolved* (see Figure 1), in that case, the flux suppression by a crazy massive black hole will result in a distinct dip in the central image which can be used to distinguish the two. Rusin Keeton Winn 2005

9) we note that the constraints in this case will be of similar strength to those of Winn 2004.

10) in the case of very small core, and a massive black hole (no detection of the image) we only get an upper limits of $\sim$ and $\sim$ for the two.

11) and in case with massive core and massive black hole we measure both with high significance. 12) we note that all these parameter combinations are plausible choices, and therefore long observations such as these will be able to either measure these parameters with confidence or place strong constraints on them.

4. CONCLUSION

REFERENCES

Barnes, J. E., & Hernquist, L. 1992, ARA&A, 30, 705
Begelman, M. C., Blandford, R. D., & Rees, M. J. 1980, Nature, 287, 307
Bussmann, R. S., Pérez-Fournon, I., Amber, S., et al. 2013, ApJ, 779, 25, 1309.0836
Ebisuzaki, T., Makino, J., & Okumura, S. K. 1991, Nature, 354, 212
Evans, N. W., & Hunter, C. 2002, ApJ, 575, 68, astro-ph/0204206
Ferrarese, L., & Merritt, D. 2000, ApJ, 539, L9, astro-ph/0006053
Ferrarese, L., Côté, P., Jordán, A., et al. 2006, ApJS, 164, 334, astro-ph/0602297
Gebhardt, K., Bender, R., Bower, G., et al. 2000, ApJ, 539, L13, astro-ph/0006289
Golse, G., & Kneib, J.-P. 2002, A&A, 390, 821, astro-ph/0112138
Hezaveh, Y., Dalal, N., Holder, G., Kisner, T., & Kuhlen, M. 2014, ArXiv e-prints, 1403.2720
Hezaveh, Y. D. 2014, ApJ, 791, L41, 1408.3631
Hezaveh, Y. D., Marrone, D. P., Fassnacht, C. D., et al. 2013, ApJ, 767, 132, 1303.2722
Inada, N., Oguri, M., Keeton, C. R., et al. 2005, PASJ, 57, L7, astro-ph/0503310
Keeton, C. R. 2003, ApJ, 582, 17, astro-ph/0206243
Kormendy, J., & Bender, R. 2009, ApJ, 691, L142, 0901.3778
Kormendy, J., & Ho, L. C. 2013, ARA&A, 51, 511, 1304.7762
Kormendy, J., & Richstone, D. 1995, ARA&A, 33, 581
Negrello, M., Hopwood, R., De Zotti, G., et al. 2010, Science, 330, 800, 1011.1255
Rocha, M., Peter, A. H. G., Bullock, J. S., et al. 2013, MNRAS, 430, 81, 1208.3025
Thomas, J., Saglia, R. P., Bender, R., Erwin, P., & Fabricius, M. 2014, ApJ, 782, 39, 1311.3783
Tremaine, S., Gebhardt, K., Bender, R., et al. 2002, ApJ, 574, 740, astro-ph/0203468
Vieira, J. D., Crawford, T. M., Switzer, E. R., et al. 2010, ApJ, 719, 763, 0912.2338
Vieira, J. D., Marrone, D. P., Chapman, S. C., et al. 2013, Nature, 495, 344, 1303.2723
Wallington, S., & Narayan, R. 1993, ApJ, 403, 517
Weiß, A., De Breuck, C., Marrone, D. P., et al. 2013, ApJ, 767, 88, 1303.2726
Winn, J. N., Rusin, D., & Kochanek, C. S. 2004, Nature, 427, 613, astro-ph/0312136